A nonlinear optical study of Frenkel excitons in Langmuir-Blodgett films

Terpstra, Jacob; Fidder, Henk; Wiersma, Douwe A.

Published in:
Chemical Physics Letters

DOI:
10.1016/0009-2614(91)85165-S

Publication date:
1991

A nonlinear optical study of Frenkel excitons in Langmuir–Blodgett films

Jacob Terpstra, Henk Fidder and Douwe A. Wiersma

Ultrafast Laser and Spectroscopy Laboratory, Department of Chemistry, University of Groningen, Nijenborgh 16, 9747 AG Groningen, The Netherlands

Received 3 January 1991; in final form 7 February 1991

We report results of a nonlinear optical investigation of the J-band of pseudoisocyanine iodide in a Langmuir–Blodgett film. The spectral narrowing of the fluorescence compared to the absorption spectrum at 77 K is ascribed to exciton relaxation in a disordered band. Resonance Rayleigh scattering and accumulated photon-echo experiments show that the exciton dephasing rate increases rapidly at energies above the renormalized band edge. This effect is linked to a change in localization of the excitons. At 1.5 K, the system's disorder is found to be larger, which leads to greater localization of the excitons. Monte Carlo calculation of the J-band's line shape at several temperatures supports the interpretation given.

1. Introduction

The possibility of using molecular materials in optical devices has greatly stimulated nonlinear optical research of thin organic films [1,2]. In this branch of science, sometimes designated as *molecular electronics*, the emphasis is on the design of molecules and polymers for special purposes, as information storage or frequency doubling, and on the fabrication and testing of thin films of these materials. These films are usually made by epitaxial growth [3] or by using the Langmuir–Blodgett (LB) technique [4,5].

While much of the ongoing research concerns the measurement and optimization of macroscopic optical parameters, there is a definite need for detailed understanding of the underlying microscopic phenomena. Grasp of the optical dynamics of the states that resonantly enhance the measured optical effects seems to be especially crucial for further optimization of these photonic materials.

We have recently initiated [6–9] a nonlinear optical investigation of aggregates in glasses and thin films. Pioneering work on LB films, using classical spectroscopic methods, has previously been done by Möbius and Kuhn [4,10]. From a study of the efficiency of energy transfer between monolayers of different J-aggregates, they concluded that the excitation is delocalized over a certain domain. They showed further that the size of the domain depends on the temperature, and that the excitation propagates over large distances on the film. Direct support for the suggestion that aggregate excitations are delocalized was recently provided by fluorescence-lifetime measurements on aggregates of pseudoisocyanine bromide (PIC-Br) in a glass [8]. These measurements showed that at low temperatures (<50 K), the *radiative* lifetime of the aggregate's excited state is about 70 ps resulting from cooperative emission of about 100 molecules. Theoretical [11–14] and experimental [6–9] studies of this *superradiant* behaviour showed that the *coherence* volume of the exciton is limited by disorder at low temperature and by exciton–phonon scattering at higher temperatures. Recent Monte Carlo calculations of the PIC system demonstrated that the J-band in these aggregates can be described as a transition to a one-dimensional disordered Frenkel exciton band [13]. Earlier Monte Carlo calculations by Schreiber and Toyozawa [14] indicated that for excitonic systems of all dimensions, states near the bottom of the band are pseudo-localized, carrying giant oscillator strength. They also showed that the Urbach absorption tail can be used as a probe for the strength of the electron–phonon coupling and for the dimen-

0009-2614/91/$ 03.50

sionality of the system. Inoue [15] was the first to use these findings to characterize the exciton–phonon interaction in LB films of a merocyanine dye.

In this Letter, we report the first results of a nonlinear optical study and Monte Carlo calculation of exciton dynamics in a PIC LB film. Results of resonance Rayleigh scattering, picosecond photon-echo and fluorescence measurements will be presented and discussed. The use of resonance Rayleigh scattering and photon echo for the study of exciton dynamics in an LB film presents a novelty. Our experiments clearly show that disorder in the film has a substantial effect on the exciton dynamics and that excitons below the renormalized band edge are more localized than above this edge. Monte Carlo calculation of the band structure and line shape of these aggregates shows that the line shape is little affected but the exciton's coherence volume is substantially affected by interchain interactions. The observed nonexponentially of the fluorescence decay at all temperatures is attributed to a combination of exciton transport and radiative decay.

2. Experimental

Pseudoisocyanine iodide (PIC-I) was obtained from Kodak and used without further purification. LB films or PIC-I were made using the adsorption method [5]. Doubly distilled water was used for the subphase (pH 8, $T=20°C$) in which PIC-I was dissolved at a concentration of 10^{-4} M. After drop-wise addition of a 1.5×10^{-3} M solution of arachidic acid in chloroform, a PIC layer is formed by adsorption to the arachidic acid monolayer. Hereafter, the two layers were transferred at a ratio of about one to hydrophobic glass slides at a pressure of 30 mN/m^2. The glass slides had been made hydrophobic by covering them with five monolayers of arachidic acid.

Resonance-Rayleigh-scattering (RRS) experiments on PIC-I in a bilayer LB film were performed with a synchronously pumped picosecond dye laser using sodium fluorescein or rhodamine-6G as a lasing dye. The Rayleigh scattering was collected at right angles with respect to the exciting beam and detected using a Spex 1402 double monochromator equipped with a RCA C31034A-02 single-photon counting tube or an amplified OMA system (Princeton Instruments) with a Spex 1877 triple-mate monochromator. Excitation intensities of less than 10^8 photons per pulse cm^{-2} were used. Fluorescence-lifetime measurements were performed with a single-photon counting system having a system response of 35 ps. The cavity dump rate was 94 kHz and the excitation wavelength was 565 nm. Intensity-dependent measurements were performed on the double-layer PIC samples at temperatures ranging from 1.5 to 298 K. These measurements show no intensity dependence with excitation densities ranging from 5×10^9 to 1.5×10^{12} photons/pulse cm^{-2}. In most measurements, an excitation density of about 10^{11} photons/pulse cm^{-2} was used. Accumulated picosecond photon-echo experiments, using stochastic excitation with a bandwidth of about 3 nm, were performed as described in ref. [6]. The results obtained were independent of the excitation intensities used, in the range of 1.5×10^{11} to 13×10^{11} photons per pulse cm^{-2}.

Monte Carlo calculations were performed as described elsewhere [13].

3. Results and discussion

Fig. 1 shows the absorption and emission spectra of a bilayer of PIC-I in the vicinity of the J-band at 77 K. Around 520 nm, another much weaker band

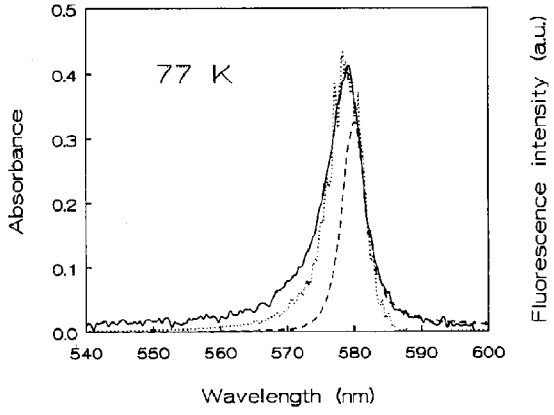

Fig. 1. Absorption (—) and emission (---) spectra of a bilayer LB film of PIC-I in the vicinity of the J-band at 77 K. The fluorescence excitation wavelength was 514.5 nm. The dotted curve presents the calculated absorption spectrum based on eq. (1) and parameters given in the text.

is observed in the absorption spectrum, which is attributed to remnant monomer absorption. The most noteworthy feature of fig. 1 is that it shows that the emission spectrum is narrowed and red-shifted compared to the absorption spectrum. Following our earlier work on aggregates of PIC-Br in a glass [13], we interpret this red-shifted emission spectrum in terms of exciton emission from a disordered band. The narrowing of the emission arises from a competition between exciton relaxation and radiative decay and the apparent red-shift of the emission spectrum is due to the fact that emission mainly occurs from states near the bottom of the exciton band.

For a better understanding of exciton dynamics in disordered systems, we need to present some theoretical background: The effects of disorder on the exciton dynamics has been dealt with by many researchers either by using a perturbational approach [11,16,17] or by numerical Monte Carlo calculations [14]. The Hamiltonian that describes the exciton dynamics in the presence of disorder, but in the absence of phonons, has the following form [11,16–18]:

$$\mathbf{H}_{ex} = \sum_n (\langle\epsilon\rangle + D_n) a_n^+ a_n + \sum_{m,n} J_{mn} a_m^+ a_n \,. \qquad (1)$$

In eq. (1), $a^+(a)$ creates (annihilates) an electronic excitation of energy $(\langle\epsilon\rangle + D_n)$ at site n. D_n represents the inhomogeneous shift from the average molecular excitation energy $\langle\epsilon\rangle$. J_{mn} designates the dipolar coupling between molecules m and n.

Note that for $D_n = 0$, eq. (1) is the Hamiltonian for a homogeneous Frenkel exciton. The presence of disorder leads to *renormalized* excitonic states, whose coherence volume critically depends on the ratio κ of the spread in disorder energies (D) and the nearest-neighbour coupling term (J_{12}). It has been shown that the Hamiltonian in eq. (1) leads, for excitonic systems of all dimensions, to the following effects:

(1) A shift of the exciton band edge to lower energy, depending on D and J_{12}. Following Schreiber and Toyozawa [14], we shall refer to this shifted exciton band edge as a *renormalized* band edge.

(2) The presence of states below the renormalized band edge carrying giant oscillator strength, which are more localized than states above this edge [14]. In absence of dephasing, these pseudo-localized states below the band edge are superradiant.

(3) An asymmetric excitonic line shape with a high-energy side that can be described by a Lorentzian [17].

(4) A steeply descending Urbach-tail (low-energy side of the absorption line shape), from which information on the exciton–phonon coupling strength can be obtained [14].

We note that in the calculations leading to the above results, it has been assumed that the dipole-allowed level is at the bottom of the band for the homogeneous system.

We now return to a discussion of the spectra shown in fig. 1 and note that the high-energy wing of the absorption spectrum indeed fits nicely to a Lorentzian, with a half-width of 120 cm^{-1}. Via a perturbational approach to the exciton's line shape, this width may be attributed to disorder-induced "scattering" of the *homogeneous* dipole-allowed exciton across the exciton band. We emphasize that the 22 fs time-constant associated with this effect should not be attributed to exciton–phonon scattering. More insight into the physics of the Lorentzian tail is obtained from numerical calculations based on a linear exciton model with random Gaussian disorder. In these Monte Carlo calculations, the site transition dipole was assumed to be aligned along the chain axis. The dotted curve in fig. 1 corresponds to the absorption spectrum calculated with a value of κ for the ratio of D/J_{12} of 0.42. The red-shift of the renormalized band edge was calculated to be 70 cm^{-1}.

Fig. 2 shows the frequency dependence of the Rayleigh intensity for near-resonance excitation of PIC-I in a bilayer at 77 K. For comparison, the absorption spectrum at this temperature is also displayed. Hegarty et al. [19] were the first ones to show that for inhomogeneously broadened excitonic transitions in quantum well structures, the resonance Rayleigh scattering can be very intense. The large efficiency of this effect was attributed to spatial fluctuations in the refractive index, caused by the fact that excitons from different regions in the sample absorb at the same frequency, while strong dispersion exists near the excitonic transition. We conclude that the same physics applies to excitons in molecular aggregates.

In case the homogeneous width is much less than the inhomogeneous width, the intensity of the Rayleigh scattering can be expressed as

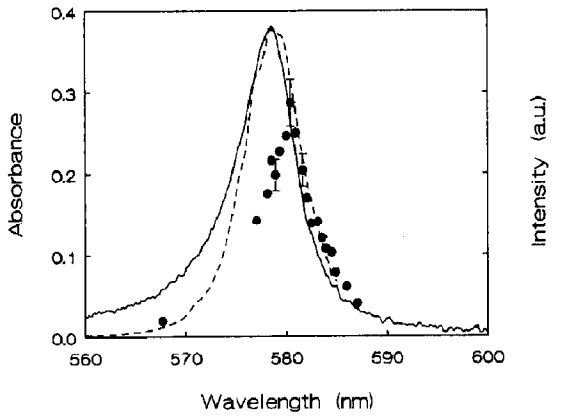

Fig. 2. Comparison between the absorption spectrum (—), the frequency dependence of the resonance-Rayleigh-scattering intensity (●), and the quantity $[1-\exp(-2\alpha(\omega)d)]\mu^2(\omega)$ (---) for a bilayer of PIC-I at 77 K.

$$I_{RS}(\omega) \propto K[1-\exp(-2\alpha(\omega)d)]\mu^2(\omega)T_2(\omega)\,. \tag{2}$$

Here, $\alpha(\omega)$ is the absorption coefficient, d the sample thickness, $\mu(\omega)$ and $T_2(\omega)$ are the frequency-dependent transition moment and dephasing time constant, respectively, and K is a constant.

Eq. (2) shows that the Rayleigh scattering can be frequency dependent either by the transition moment or the dephasing time constant. The result of a numerical calculation of the quantity $[1-\exp(-2\alpha(\omega)d)]\mu^2(\omega)$ for the J-band in the PIC bilayer is also presented in fig. 2. From this figure, we conclude that the collapse of the Rayleigh intensity on the high-energy side of the spectrum is mainly caused by a shortening of the dephasing time constant T_2 in this energy region. Excitons above the renormalized band edge thus dephase much faster than those below the edge. Comparison of figs. 1 and 2 also shows that the frequency dependence of the Rayleigh scattering looks like the fluorescence spectrum at 77 K. Because the fluorescence spectrum results from a competition between intraband exciton relaxation and radiative decay, the correspondence between the fluorescence and Rayleigh-scattering spectra at 77 K suggests that, at this temperature, optical *dephasing* ($T_2(\omega)$) is dominated by population relaxation. An important conclusion we may draw then is that excitons below the renormalized band edge are more localized than excitons above this edge.

Fig. 3 shows the low-temperature absorption, emission and Rayleigh-scattering intensity spectrum of the PIC-bilayer. From an inspection of figs. 1 and 3, we infer that the absorption spectrum at 1.5 K is substantially broader than at 77 K. We conclude that the disorder in the aggregate is larger at low temperature. Monte Carlo simulation of the line shape shows that a reasonable fit can be obtained for a κ of 0.58. From the fact that upon warming the sample from 1.5 K to room temperature and cooling to 77 K, the absorption spectrum regains nearly its original line shape at this temperature, we suggest that the increased disorder at 1.5 K is due to a difference in expansion coefficient of the film and the substrate. Further, note that the resonance Rayleigh intensity spectrum at 1.5 K is much broader than at 77 K. The conclusion is that the larger disorder at 1.5 K causes the excitons to be more localized at 1.5 K than at 77 K. Numerical calculations confirm this idea and will be published elsewhere. Fig. 3 also shows that at 1.5 K, the emission spectrum is red-shifted compared to the resonance Rayleigh intensity spectrum.

To obtain quantitative information regarding the exciton dynamics, we performed accumulated photon-echo experiments at 1.5 K. The results of these experiments at three different wavelengths are shown in fig. 4. Single-exponential fits to these decays yield photon-echo lifetimes ($\frac{1}{2}T_2$) of 3.2 ± 0.2 ps (582.5 nm), 2.2 ± 0.2 ps (578.5 nm) and 1.0 ± 0.2 ps (576 nm). Note that the apparent rise of the echo signal

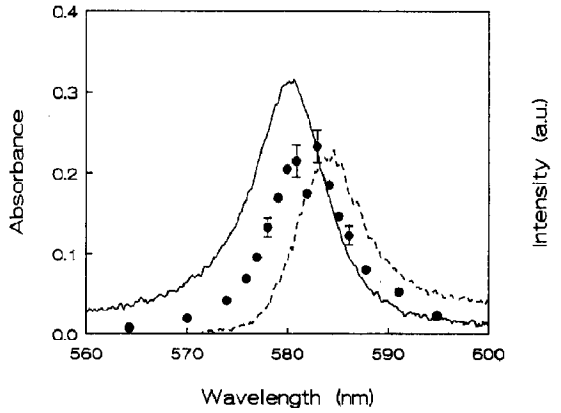

Fig. 3. Absorption (—) and emission (---) spectra and frequency dependence of the resonance-Rayleigh-scattering intensity (●) of a bilayer of PIC-I at 1.5 K.

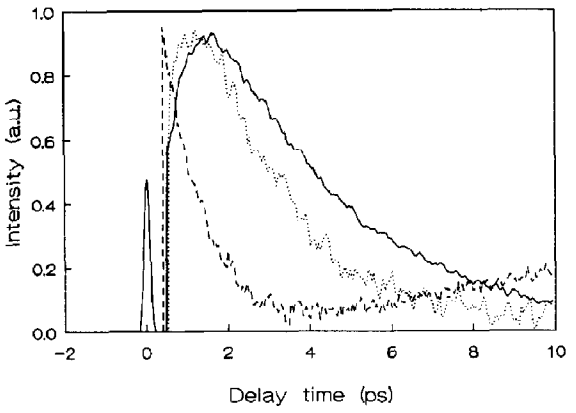

Fig. 4. Accumulated photon-echo decays at 1.5 K from a bilayer of PIC-I at excitation wavelengths: 582.5 nm (—), 578.5 nm (···) and 576.0 nm (---). The corresponding decay times are given in the text. The signal at $t=0$ caused by interference of pump and probe scattered light has been omitted. The peak at $t=0$ is the field autocorrelation of the stochastic excitation pulses.

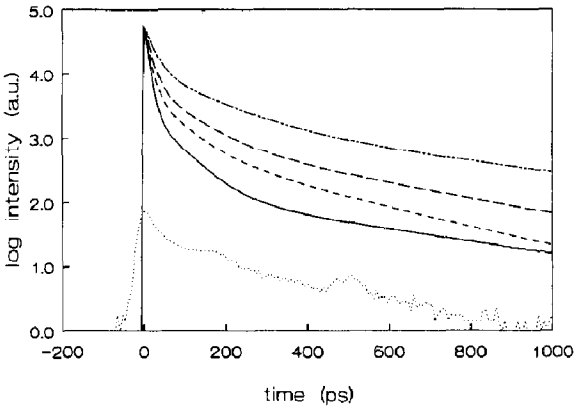

Fig. 5. Wavelength dependence of the fluorescence decay of a bilayer LB film of PIC-I at 1.5 K. The decay times (initial height) of the fast component of the deconvoluted decay curves are 9 ps (0.96) at 574 nm (—); 11 ps (0.91) at 581 nm (---); 14 ps (0.89) at 584 nm (---) and 21 ps (0.81) at 589 nm (----). The dotted curve represents the instrument response.

at delay times over 4 ps for 576 nm excitation is due to an underlying incoherent pump–probe signal. These results confirm the conclusion of the Rayleigh-scattering experiments that T_2 decreases rapidly above the band edge. At 77 K, photon-echo measurements were possible at the absorption peak only and gave a decay time of 500 fs. These data in combination with the measured frequency dependence of the Rayleigh scattering can be used to obtain $T_2(\omega)$ over the whole spectrum. It seems worth mentioning that this is the first report of any photon echo generated in an LB film.

Finally, we show in fig. 5 some deconvoluted fluorescence-decay curves at 1.5 K, detected at different emission wavelengths. The decays are nonexponential and to obtain a good fit, at least three different exponentials are needed. From these fits, the initial decays are found to change from 21 ps to 9 ps for detection at 589 nm and 574 nm, respectively. We notice that the 21 ps initial decay, which is presumed to be dominated by radiative decay [20], is about a factor of three shorter than was observed for the J-band of PIC-Br in a glass. Lifetime measurements on the PIC-bilayer have further shown that the initial decay of the fluorescence is much faster at 77 K than at 1.5 K. Relative fluorescence quantum-yield measurements indicate that this feature is caused by a lowering of the quantum yield with rising temperature. The time-resolved emission spectra in these LB films are clearly determined by both radiative and radiationless decay of the excitons. However, more work needs to be done to obtain a full understanding of the exciton dynamics in LB films.

Acknowledgement

We are indebted to F. de Haan for providing the programs for instrument control and data analysis. We also thank Dr. A.J. Schouten of the Polymer Chemistry Group for use of the LB-film growth facility and advice for making the samples. We gratefully acknowledge stimulating discussions with Dr. K.E. Drabe on Rayleigh scattering in aggregates. The investigations were supported by the Netherlands Foundation for Chemical Research (SON) and Physical Research (FOM) with financial aid from the Netherlands Organization for the Advancement of Science (NWO).

References

[1] E. Hanamura, Phys. Rev. B 37 (1988) 1273.
[2] Y. Wang, Chem. Phys. Letters 126 (1986) 209.
[3] S.E. Rickert, J.B. Lando and S. Ching, in: ACS Symp. Ser. 233. Nonlinear optical properties of organic and polymeric materials (American Chemical Society, Washington, 1983) ch. 11.

[4] H. Kuhn, D. Möbius and H. Bücher, in: Techniques in chemistry, Vol. 1, Part IIIB (Wiley-Interscience, New York, 1972) pp. 577ff.
[5] U. Lehmann, Thin Solid Films 160 (1988) 257.
[6] S. de Boer, K.J. Vink and D.A. Wiersma, Chem. Phys. Letters 137 (1987) 99.
[7] S. de Boer and D.A. Wiersma, Chem. Phys. 131 (1989) 135.
[8] S. de Boer and D.A. Wiersma, Chem. Phys. Letters 165 (1990) 45.
[9] H. Fidder, J. Knoester and D.A. Wiersma, Chem. Phys. Letters 171 (1990) 529.
[10] D. Möbius and H. Kuhn, Israel J. Chem. 18 (1979) 375.
[11] F.C. Spano and S. Mukamel, J. Chem. Phys. 91 (1989) 683.
[12] F.C. Spano, J.R. Kuklinski and S. Mukamel, Phys. Rev. Letters 65 (1990) 211.
[13] H. Fidder and D.A. Wiersma, submitted for publication; H. Fidder, J. Terpstra and D.A. Wiersma, submitted for publication.
[14] M. Schreiber and Y. Toyozawa, J. Phys. Soc. Japan 51 (1982) 1528, 1537.
[15] T. Inoue, Thin Solid Films 132 (1985) 21.
[16] E.W. Knapp, Chem. Phys. 85 (1984) 73.
[17] J. Klafter and J. Jortner, J. Chem. Phys. 68 (1978) 1513.
[18] P.W. Anderson, Phys. Rev. 109 (1958) 1492.
[19] J. Hegarty, M.D. Sturge, C. Weisbuch, A.C. Gossard and W. Wiegmann, Phys. Rev. Letters 49 (1982) 930.
[20] H. Gruhl, H.-P. Dorn and K. Winzer, Appl. Phys. B 38 (1985) 199.